An explanation for the non-monotonic temperature dependence of the photoluminescence spectral features of self-organized InAs QDs

Rayhani Jawher, Mehrez Oueslati, Vincent Sallet, Jean-Christophe Harmand, Radhwen Chtourou

An explanation of the non-monotonic temperature dependence of the photoluminescence spectral parameters of self-organized InAs QDs

Rihani Jawher[a,*], Mehrez Oueslati[b], Vincent Sallet[c], Jean-Christophe Harmand[d], and Radhwen Chtourou[a]

[a]Laboratoire de Photovoltaïque de Semiconducteurs et de Nanostructures, Centre de Recherche des Sciences et Technologie de l'Energie, BP. 95, Hammam-Lif 2050, Tunisia.

[b]Laboratoire de Nanomatériaux, Nanotechnologie et Energie (L2NE), Faculté des Sciences de Tunis, Université de Tunis El Manar, 2092 Tunis, Tunisia.

[c]Groupe d'Etude de la Matière Condensée (GEMAC), CNRS, Université St Quentin en Yvelines, Université Paris-Saclay, 45 avenue des Etats-Unis, 78035 Versailles, France.

[d] C2N, Centre de Nanosciences et de Nanotechnologies, Université Paris-Saclay, CNRS, UMR 9001, 91120, Palaiseau, France

Abstract:

Temperature-dependent photoluminescence (**PL**) measurements under different excitation densities were performed on self-assembled InAs quantum dots (**QDs**) grown by molecular beam epitaxy. Non-monotonic evolutions in the curves of the PL spectral parameters as a function of the sample temperature were observed in the low-temperature regime. In fact, the PL peak energy of the QDs shows a sigmoidal variation with increasing temperature. This component is accompanied by an anomalous increase in the integrated intensity over the temperature range of 8 to 50K. These optical behaviors have been attributed to the emission from deep states that exist in the potential of the dots. A very simple rate equation model, which describes the thermally activated emission and trapping of photo-injected carriers, is proposed to illustrate the interpretations made regarding the evolution of the integrated PL intensity with increasing temperature. A good agreement between the model simulation of the integrated PL intensity and the experimental results was obtained for temperatures ranging from 8 to 300K. It was found that the thermally activated process of the intra-dot redistribution of carriers provides a good description of the anomalous behaviors encountered in the PL investigations depending on the temperature of the QD sample.

[*]Corresponding author. Tel : +21697669764 ; fax : + 21679325825.

E-mail: rihani_jaouher@yahoo.fr

I. Introduction:

Over the past decade, QD semiconductor materials have attracted considerable attention due to their prominent applications in the design of memory devices and single-photon emitters [1-3]. The main physical property of these materials is to have all the photo-carriers distributed among discrete levels, which drastically ameliorates the electronic and optical efficiencies of the optoelectronic devices and intermediate band solar cells [4-6]. On the other hand, in order to attain high power conversion efficiency in QD-based photovoltaic systems, the photo-excitation inside the solar cell structures must be extended [7, 8]. However, the efficiency of solar cells is found to be reduced due to some unanticipated thermal effects of the photo-carriers inside the QDs (such as the relaxation and non-radiative recombination paths related to the carriers trapped in deep levels). Understanding the thermal carrier dynamics inside the self-organized QD structures is thus crucial for improving the performance of QD-based photovoltaic systems [9].

It is commonly stated that the anomalous blue-shift of the PL peak energy of the QDs with increasing temperature is assigned to the presence of deep localized states (**LS**) within the QD structure [10]. For the self-organized InAs/GaAs QDs system, this blue-shift of the dot-luminescence energy generally occurs at temperatures below 70K [11, 12], which is much smaller than the characteristic temperature (~ 120 K) of the onset of the thermal quenching of the PL intensity of the dots [13]. Due to the presence of such trap levels in the QD semiconductor materials, the conventional semi-empirical models of Varshni [14] and Fan [15] are unable to reproduce the sigmoidal variations (S-shape feature) that may appear in the temperature dependence of the PL peak energy, and therefore they cannot provide satisfactory values of the fitting parameters [11]. In the literature, several semi-empirical models have been proposed to account for the blue-shift of the PL peak energy with increasing temperature [16-18]. Eliseev et al. [16] have proposed the band-tail model which can replicate, at high temperatures, the “S-shaped” temperature dependence of the PL peak position for nitrogen-based semiconductor heterostructures. More recently, Li et al. [17] have proposed the localized-state ensemble model which has been widely employed in several III–V semiconductor nanostructures to explain the anomalous deviation from Varshni’s equation of the bandgap shrinkage depending on the temperature [12, 19]. Very recently, by including the contribution of localized states, Dixit et al. [18] have proposed a modified Varshni expression, which was adapted to reproduce the anomalous temperature dependency of the PL peak energy and also to provide an accurate determination of the exciton localization energy in

bulk and quantum well structures. However, possible explanations based on the study of the temperature dependence of the PL intensity of the dots and which consider the contribution of the LS are rarely encountered in the literature, especially for self-assembled InAs/GaAs QD systems. In this work, the carrier dynamics inside the investigated QD structure are discussed qualitatively and quantitatively in order to explain the observed sigmoidal variation of the dot-luminescence intensity as a function of the temperature.

II. Experimental details:

The structure studied in this work contains a single layer of InAs QDs (wetting layer) sandwiched in a GaAs matrix [20]. The Stranski-Krastanov QDs were grown by molecular beam epitaxy (**MBE**) on (001)-oriented GaAs substrates. Gallium and indium fluxes were supplied from thermal effusion cells, As_2 species from a cracking source. The growth procedure for the QDs deposition is the following. First, a 0.3 µm thick GaAs buffer was grown at 600 °C with a rate of 0.2 nm/s. Subsequently, the substrate temperature was decreased to 490°C in order to allow deposition of the wetting layer (**WL**). The thickness of the deposited InAs was fixed to 2.4 monolayers with a growth rate of 0.04 nm/s. A 100 nm thick GaAs cap was immediately grown after, while the growth temperature was increased to 600 °C. Photoluminescence measurements were carried out using a closed-cycle He cryostat and a 514.5-nm line of an Ar^+ laser. Optical spectra were collected with a $f = 0.25$ m spectrometer with a 1200 l/mm grating and focused onto a cooled GaInAs photodiode detector.

III) Results and discussion:

Figure 1 depicts the PL spectra of the QD sample recorded in the 8-300K temperature range under several excitation densities. Using a Gaussian fitting analysis, the evolutions of the integrated PL intensity and the PL peak energy as a function of the temperature are determined from the fitting results and are shown in figures 2a and 2b, respectively. It can be clearly seen from Fig. 2 that the PL peak energy (**PLPE**) of the QDs exhibits an anomalous blue-shift when the temperature grows up from 8K to T_S (temperature of turning out to red-shift of the PLPE). At the same time, the integrated PL intensity (**IPLI**) of the dots exhibits an abnormal enhancement in the low-temperature region (see Fig. 2b). As was stated in our previous study, this abnormal dependence on the temperature of the PL spectral parameters has been assigned to the coexistence of deep LS with the intrinsic electronic levels of the dots [20]. It should be emphasized that the existence of spatially localized deep trap levels in

MBE-grown In(Ga)As/GaAs QDs has been clarified to be caused by point defects (such as chemical impurities, interstitials, and vacancy defects), which are introduced by the lattice mismatch strain during the growth process of In(Ga)As on GaAs [21-23]. Such deep trap levels may lie energetically below or above the ground states (**GS**) of the dots [21, 24]. Their density of states has been shown to be one or more orders of magnitude smaller than the total density of the dot ground states [22, 23]. The absolute value of the energy spacing ($\Delta\varepsilon$) between the LS and the GS is often defined as the localization energy of the deep-trap levels. Like the Fermi level in the Fermi-Dirac distribution, $\Delta\varepsilon$ constitutes a specific energy below which the LS will be occupied by carriers at 0K [17, 19]. Note that the value of $\Delta\varepsilon$ is generally different from that of the energy separation between the maximum and the minimum of the PLPE recorded in the [8K, T_S] temperature range (see Fig. 2a) [18]. In the following, a study of the thermal dynamics of carriers involved in the investigated QD structure is presented to explain the anomalous tendencies in the spectral parameters that are observed in the temperature-dependent PL measurements.

Fig. 2 shows that the temperature dependence of the PL intensity and the bandgap energy of the dots exhibit practically the same increasing and decreasing trend with increasing temperature. Moreover, the quenching behavior of the PL intensity practically starts at a temperature very close to the T_S value (~50K). The temperature dependence of the PL spectral parameters is therefore governed by two regimes. The first one occurs for temperatures below T_S and marks a gradual improvement of the IPLI accompanied by an anomalous blue-shit of the PL peak energy. The second regime occurs for temperatures above T_S and marks a typical reduction of the gap energy of the dots and a typical quenching behavior of their PL signal. As can be seen in Fig. 2, the dots' bandgap energy shifts immediately to the blue with the small temperature rise from 8K. According to this, the photo-generated carriers are trapped in deep localized states at very low temperatures (around 8K) [19, 22]. In addition, these trapped carriers are thermally activated towards the upper states [19, 22]. However, the T_S temperature, which characterizes the turning out to red-shift of the PLPE, remains almost unchanged with the increase in the excitation density (see Fig. 2a). This implies that the T_S temperature is essentially independent of the concentration of carriers injected into the QDs. Therefore, the activation energy ($\Delta\varepsilon$), for which the majority of carriers trapped in the LS are transferred to the GS, is suggested to be close to k_BT_S [10]. Similar activation energy values to k_BT_S have been reported for self-organized In(Ga)As QD systems (4 meV) by Ezidini et al.

[12] and (7 meV) by Yeo et al. [11]. In these reported works, the LS have been demonstrated to be located in the close vicinity of the QD states.

In the first regime, the re-populating of the ground states by the thermally activated carriers from the localized states can explain the anomalous blue-shift of the dot-luminescence energy seen in Fig. 2a. However, due to carrier-phonon coupling mechanisms, a rise in temperature should aggravate the non-radiative recombination channels. Even though it is believed that all the carriers trapped in the LS are transferred to the GS, the PL signal from the dots should exhibit a quenching behavior with increasing temperature. However, Fig. 2b shows that when the temperature grows from 8K to T_S, the IPLI of the dots enhances. Moreover, this improvement in the IPLI becomes considerably more significant with increasing excitation density. Similar optical observations have been reported in the literature for other QD materials [10], and it is convincing to assume that the GS should have a higher radiative recombination efficiency than that of the LS.

Taking into account of the above assumptions, a possible picture of the thermal exchange of carriers between the LS and the GS of the dots could be described as follows (see Fig. 3). Due to the coexistence of the deep trap levels with the intrinsic states of the dots, the PL signals obtained from the investigated sample correspond to the combination of the radiative emission from the LS and that from the GS [10, 19]. At a very low temperature (~ 8K), the lowest energies are preferred, so most of the photo-generated carriers are relaxed into the LS (see Fig. 3a). In the 1st regime, the gradual increase in temperature provides thermal energy to these trapped carriers, which causes them to begin populating the GS of the dots (see Fig. 3b). This intra-dot redistribution of carriers leads to the blue-shifting behavior of the PLPE seen in Fig. 2a since the LS lie below the GS. At the same time, this aspect induces a gradual enhancement of the PL intensity of the QDs since the GS are assumed to have much higher radiative recombination efficiency than that of the LS. At temperatures close to the T_S value (end of the 1st regime), the thermal activation energy $\Delta\varepsilon \approx k_B T_S$ is given for the localized carriers (see Fig. 3c). Then, most of the carriers trapped in the LS are thermally re-emitted towards the GS. In the recorded PL measurements, this aspect marks the end of the blue-shifting behavior of the PLPE seen in Fig. 2b. With a further increase in the temperature (2nd regime), the LS become a transient level that provides carriers to the GS without consumption. So, the recorded optical signals of the QD sample will only result from the GS of the dots. Then, typical evolutions of the PL spectral parameters of the QDs as a function of

the temperature should be evident (such as bandgap reduction and thermal quenching of the PL intensity).

In order to verify qualitatively the assumptions cited above, a simple coupled rate-equation model is proposed to describe the carrier relaxation dynamics involved in the studied structure. The model should explain both the anomalous enhancement and the thermal quenching of the QD PL intensity seen in the first and second regimes, respectively (see Fig. 2b). The charge carrier movements considered in the rate equation model are schematically described in Fig. 3. In continuous excitation mode, G_0 carriers per QD per second are generated in the bulk GaAs and then rapidly diffuse into the wetting layer barrier. Once in the wetting layer, the carriers are randomly captured either in the in the deep localized states (with a capture rate of T_L) or in the GS of the dots (with a capture rate of T_G). In the present PL investigations, the bulk GaAs and the barrier InAs act as intermediate levels which provide carriers to the dots without consumption since the PL spectra of the QD sample did not reveal any characteristic band of radiative emissions from the bulk and wetting layer materials. Furthermore, the absence of PL emissions from the excited states of the QDs under the low excitation levels used in our experiments suggests that the dots are occupied by a single charge carrier located in the lowest states of the QDs [25, 26]. The correlation between carriers involved in the capture and in the thermal emission processes was neglected. This hypothesis is in some respects consistent with the one-particle model proposed by E. C. LE RU et al., which strongly suggests independent mechanisms of escape and recapture of charge carriers for self-assembled InAs/GaAs quantum dots [25]. The carriers captured by the LS and the GS can spontaneously recombine with radiative recombination rates of R_L and R_G, respectively. With the increase in temperature, the carriers injected into the localized states can be thermally re-emitted towards the GS with a recombination rate of $B(T)$ (characterized by the activation energy $\Delta\varepsilon \approx k_B T_S$). Similarly, the carriers injected into the ground states can get lost by non-radiative paths with a recombination rate of $N_R(T)$ (characterized by an activation energy of E_a). The terms describing the thermal emission of carriers from the LS and GS are $B(T) = b\, exp(-\Delta\varepsilon/kT)$ and $N_R(T) = n_r\, exp(-E_a/kT)$, respectively. $\Delta\varepsilon$ and E_a are the needed activation energies for carriers to escape from the LS and GS, respectively. The charge carrier movements under steady-state conditions are as follows (see Fig. 3):

WL Barrier: $$G_0 - T_L n_W - T_G n_W = \frac{dn_W}{dt} = 0 \qquad (1)$$

LS: $T_L n_W - R_L n_L(T) - B(T) n_L(T) = \frac{dn_L}{dt} = 0$ (2)

GS: $T_G n_W - R_G n_G(T) - N_R(T) n_G(T) + B(T) n_L(T) = \frac{dn_G}{dt} = 0$ (3)

Where n_W, n_L and n_G are the concentrations of carriers in the WL barrier, LS, and GS, respectively.

Eq. (1) can be transformed into:

$G_L = T_L n_W = \frac{T_L G_0}{T_L + T_G}$ (4) and $G_G = T_G n_W = \frac{T_G G_0}{T_G + T_L}$ (5)

Where G_0, G_L and G_G are the generation rates of carriers in the WL barrier, LS, and GS, respectively.

Eq. (2) transforms into: $n_L(T) = \frac{G_L}{R_L + B(T)}$ and so $R_L n_L(T) = \frac{R_L G_L}{R_L + B(T)}$ (6)

Eq. (3) transforms into: $n_G(T) = \frac{G_G + B(T) n_L(T)}{R_G + N_R(T)}$ (7)

By combining Eqs. (4), (5) and (7), the IPLI can be written as:

$$I_{PL}(T) = \frac{R_G}{\{R_G + N_R(T)\}} \times n_G(T) = \frac{G_G}{R_G\left\{1 + \frac{N_R(T)}{R_G}\right\}^2} \times \left\{1 + \frac{G_T}{G_G} \times \frac{1}{1 + \frac{R_L}{B(T)}}\right\} \quad (8)$$

Considering that: $N_R(T) = n_r \, exp(-E_a/kT)$ and $B(T) = b \, exp(-\Delta\varepsilon/kT)$

From these expressions and with the assumption that $\Delta\varepsilon \approx k_B T_S$, Eq. (8) can be transformed into:

$$I_{PL}(T) \propto \frac{G_G}{\left\{1 + \frac{n_r}{R_G} \times exp(-E_a/kT)\right\}^2} \times \left\{1 + \frac{G_T}{G_P} \times \frac{1}{1 + \frac{R_L}{b} \times exp(T_S/T)}\right\} \quad (9)$$

To simplify the rate equations, a considerable approximation is made. The luminescent states of the dots are assumed to have an identical capture efficiency of the charge carriers ($T_G \approx$

T_L). This assumption is supported by the commonly used random capture processes of carriers by the QD states for an average occupancy in the dots much smaller than one e-h pair [25, 26]. So given that $\frac{G_L}{G_G} = \frac{T_L}{T_G} \approx 1$ and with the assumption that $I_{PL}(8K) \approx I_{PL}(0K) = G_G$, the IPLI data of the dots could be fitted with the following law:

$$I_{PL}(T) \propto \frac{I_{PL}(8K)}{\{1 + A \times exp(-B/kT)\}^2} \times \left\{1 + \frac{1}{1 + C \times exp(T_S/T)}\right\} \qquad \text{(I)}$$

Where $A = \frac{n_r}{R_G}$, $B = E_a$ and $C = \frac{R_L}{b}$ are the fitting parameters.

Figure 4 exhibits the fit of the experimental data with the help of the Eq. (I) using different excitation densities. The fitting results obtained using such equation are summarized in Tab. 1. The data adjustment with the Arrhenius formula [27] (expressed as $I_{PL}(T) = \frac{I_{PL}(0)}{1 + L_1.T^{3/2} + L_2.T^{3/2} \times exp\{-(E_a/kT)\}}$, where L_1, L_2 and E_a are the fitting parameters) is also added to this figure. As shown in Fig. 4, the temperature dependence of the integrated PL intensity of the dots cannot be replicated using the Arrhenius formula. However, the Eq. (I) significantly reproduces the experimental data and therefore validates all of the above assumptions. Thus, the thermally activated process of the intra-dot redistribution of carriers provides a good description of the anomalous behaviors encountered in the PL investigations depending on the temperature of the QD sample. In fact, with the increase in temperature from 8K to T_S, the carriers trapped in the deep localized states are thermally activated towards the ground states of the dots. This results in an improvement of the PL signals and a blueshift of their peak energies. As the temperature rises from T_S, the thermal activation energy Δε is given to the localized carriers and will remote them to the GS. Then, only the radiative emissions from the GS must be taken into consideration. Subsequently (second regime), standard evolutions of the PL spectral parameters as a function of the temperature (such as the band gap reduction and the quenching of the integrated intensity) should be observable. For the InAs/GaAs QDs system, it is worth noting that the small values of the activation energy (30–60 meV) that could be obtained by fitting the PL experimental data with appropriated formulas are most likely attributed to the thermally activated capture of the photogenerated carriers (before being captured by the QDs) by nonradiative centers located at the InAs/GaAs interface and/or attributed to the thermal escape of carriers towards nonradiative centers

located nearby the QDs [28]. However, much higher activation energies (around 100 meV), such as those obtained in the present experimental results, probably correspond to the thermal escape of carriers outside the QDs towards the WL barrier [28]. Note that increasing the excitation density weakens the activation energies (see Tab. 1). This is probably in good agreement with the band-filling effect, which gives rise to shallower confinement states [10].

IV) Conclusion:

In conclusion, temperature-dependent PL measurements of self-assembled InAs/GaAs QDs grown by MBE were studied. Two characteristics of the dot photoluminescence spectra, such as the PLPE and the IPLI, have marked anomalous trends when the temperature goes from 8 to 50K. A qualitative discussion was made to explain these anomalous trends using different excitation densities in the temperature-dependent PL investigation. It is found that the blueshift of the QD emission and the enhancement of the QD photoluminescence are caused by the thermal transfer of excitons from the localized states towards the ground states of the dots. In order to verify this assumption, a simple rate-equation model was proposed to describe the carrier movements in the QD states. A good agreement between the model simulation and the experimental data is obtained and thus confirms the assumptions made on the carrier exchange between the localized states and the ground states of the dots.

References:

[1]: Johann Stachurski, Sebastian Tamariz, Gordon Callsen, Raphaël Butté, and Nicolas Grandjean, Light: Science & Applications 11:114 (2022).

[2]: Christopher F Schuck, Robert Boutelle, Kevin Silverman, Galan Moody, and Paul J Simmonds, J. Phys. Photonics, 3, 024012 (2021).

[3]: Ying Yu, Guo-Wei Zha, Xiang-Jun Shang, Shuang Yang, Ban-Quan Sun, Hai-Qiao Ni, and Zhi-Chuan Niu, National Science Review 4: 196–209 (2017).

[4]: Martin Geller, Appl. Phys. Rev. 6, 031306 (2019).

[5]: Weng W. Chow and Stephan Reitzenstein, APPLIED PHYSICS REVIEWS 5, 041302 (2018).

[6]: Xiang-Bin Su, Ying Ding, Ben Ma, Ke-Lu Zhang, Ze-Sheng Chen, Jing-Lun Li, Xiao-Ran Cui, Ying-Qiang Xu, Hai-Qiao Ni, and Zhi-Chuan Niu, Nanoscale Research Letters. 13, 59 (2018).

[7]: Han Song, Yu Lin, Zhengyan Zhang, Huashang Rao, Wenran Wang, Yueping Fang, Zhenxiao Pan, and Xinhua Zhong, Journal of the American Chemical Society, 143, 4790−4800 (2021).

[8]: Gyea Young Kwak, Tae Gun Kim, Nicholas Kim, Ji Young Shin, and Kyung Joong Kim, Journal of Nanotechnology, Volume 31, Number 19 (2020).

[9]: Shenglin Wang, Xiaoguang Yang, Hongyu Chai, Zunren Lv, Shuai Wang, Haomiao Wang, Hong Wang, Lei Meng, and Tao Yang, Journal of Photonics, 9, 290 (2022).

[10]: G. E. Weng, W. R. Zhao, S. Q. Chen, H. Akiyama, Z. C. Li, J. P. Liu, and B. P. Zhang, Nanoscale Research Letters. vol 10, n°31 (2015).

[11]: Inah Yeo, Jin Dong Song, and Jungil Lee, Applied Physics Letters 99, 151909 (2011).

[12]: M. Ezzedini, T. Hidouri, M. H. Hadj Alouane, A. Sayari, E. Shalaan, N. Chauvin, L Sfaxi, F. Saidi, A. Al-Ghamdi, C. Bru-Chevallier, and H. Maaref, Nanoscale Research Letters 12 : 450 (2017).

[13]: S. Sanguinetti, D. Colombo, M. Guzzi, E. Grilli, M. Gurioli, L. Seravalli, P. Frigeri, and S. Franchi, PHYSICAL REVIEW B 74, 205302 (2006).

[14]: Y. P. Varshni, Physica (Amesterdam) 34, 149 (1967).

[15]: H. Y. Fan, Photon-Electron Interaction, Crystals Without Fields (Springer, Berlin, 1967), p. 134.

[16]: Petr G. Eliseev, Piotr Perlin, Jinhyun Lee, and Marek Osiński, Appl. Phys. Lett. 71, 569 (1997).

[17]: Q. Li, S. J. Xu, M. H. Xie, and S. Y. Tong, EUROPHYSICS LETTERS, 71 (6), pp. 994–1000 (2005).

[18]: V. K. Dixit, S. Porwal, S. D. Singh, T. K. Sharma, S. Ghosh, and S. M. Oak J. Phys. D: Appl. Phys. 47, 065103 (2014).

[19]: S. A. Lourenço, I. F. L. Dias, J. L. Duarte, E. Laureto, V. M. Aquino, and J. C. Harmand, Brazilian Journal of Physics, vol. 37, number. 4, pp. 1212-1219 (2007).

[20]: Rihani Jawher, Mehrez Oueslati, Vincent Sallet, Jean-Christophe Harmand, and Radhwen Chtourou, Applied Surface Science Advances, 7, 100199 (2022).

[21]: S. W. Lin, C. Balocco, M. Missous, A. R. Peaker, and A. M. Song, PHYSICAL REVIEW B 72, 165302 (2005).

[22]: C. Walther, J. Bollmann, H. Kissel, H. Kirmse, W. Neumann, and W. T. Masselink, Appl. Phys. Lett. 76, 2916 (2000).

[23]: T. Asano, Z. Fang, A. Madhukar, J. Appl. Phys. 107, 073111 (2010).

[24]: A. Fiore, P. Borri, W. Langbein, J. M. Hvam, U. Oesterle, R. Houdré, R. P. Stanley, and M. Ilegems, Appl. Phys. Lett. 76, 3430 (2000).

[25] : E. C. Le Ru, J. Fack, and R. Murray, Physical Review B. 67, 245318 (2003).

[26] : V. Popescu, G. Bester and A. Zunger, Appl. Phys. Lett. 95, 023108 (2009).

[27]: [25 de M1] Mukul C. Debnath, Baolai Liang, Ramesh B. Laghumavarapu, Guodong Wang, Aparna Das, Bor-Chau Juang, Diana L. Huffaker, J. Appl. Phys. 121 (2017), 214304.

[28] : T. V. Torchynska, J. L. Casas Espinola, L. V. Borkovska, S. Ostapenko, M. Dybiec, O. Polupan, N. O. Korsunska, A. Stintz, P. G. Eliseev, and K. J. Malloy, JOURNAL OF APPLIED PHYSICS 101, 024323 (2007).

Figure captions:

Fig. 1. PL spectra of the studied sample taken at different temperatures under several excitation densities (P_{ex}). **(a)** $P_{ex} = P_0$, **(b)** $P_{ex} = 2.5 \times P_0$, **(c)** $P_{ex} = 7.5 \times P_0$, and **(d)** $P_{ex} = 15 \times P_0$.

Fig. 2a. Temperature dependence of the PL peak energy of the dots under different excitation densities. For clarity of the figure, the PL peak energy of the dots is shifted along the energy axis of 10 meV, 30 meV, and 100 meV for the excitation densities of $2.5 \times P_0$, $7.5 \times P_0$, and $15 \times P_0$, respectively.

Fig. 2b. Temperature dependence of the integrated PL intensity of the dots under different excitation densities. For clarity of the figure, the integrated PL intensity of the dots corresponding to the excitation density of $15 \times P_0$ is shifted along the intensity axis by 0.002 (u.a.).

Fig. 3. Schematic representation of the energy band diagram of the studied sample. The diagram includes the energetic location of the local states with respect to the QDs. **(a)**: At very low temperatures (around 8K). **(b)**: For temperatures between 8K and T_S. **(c)**: For temperatures above T_S.

Fig. 4. Evolution of the IPLI of the dots as a function of the temperature accompanied by the adjustment to the model described in the text and also the adjustment to the Arrhenius' law. **(a)** $P_{ex} = P_0$, **(b)** $P_{ex} = 7.5 \times P_0$, **(c)** $P_{ex} = 15 \times P_0$, and **(d)** $P_{ex} = 25 \times P_0$.

Table captions:

Table 1. Parameters obtained from the data fitting results using the model described in the text.

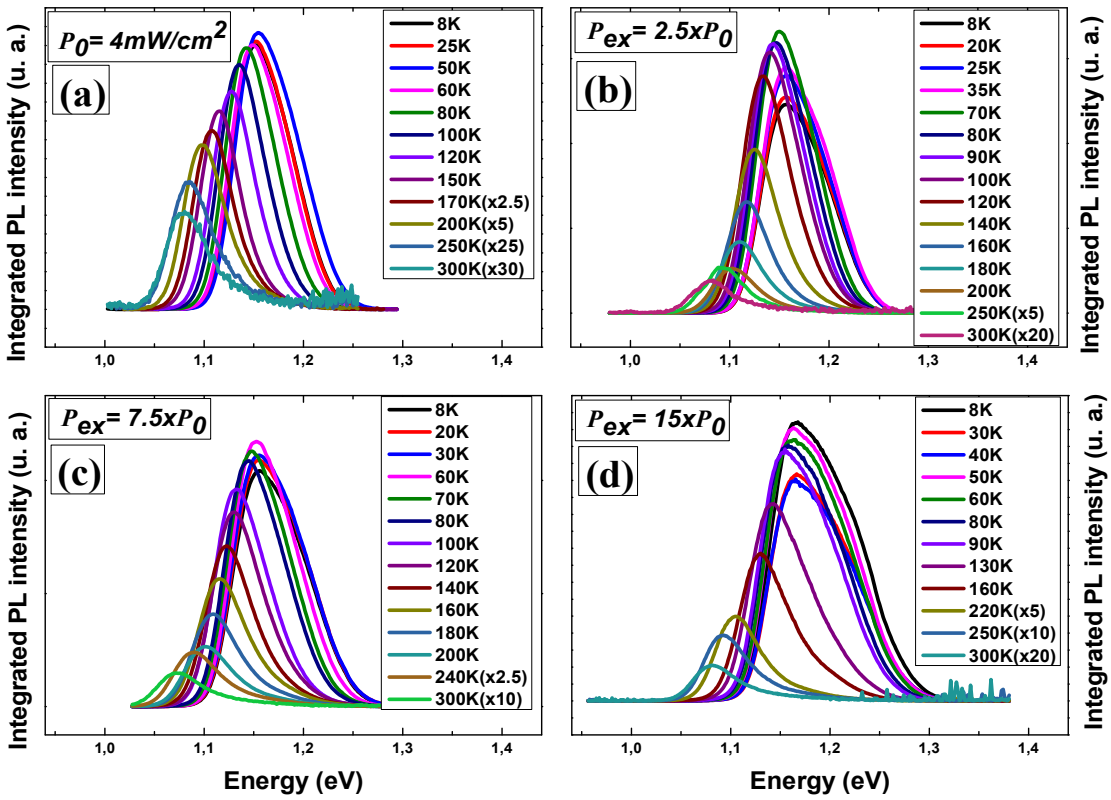
(a)
P_0= 4mW/cm^2
8K
25K
50K
60K
80K
100K
120K
150K
170K(x2.5)
200K(x5)
250K(x25)
300K(x30)
(b)
P_{ex}= 2.5xP_0
8K
20K
25K
35K
70K
80K
90K
100K
120K
140K
160K
180K
200K
250K(x5)
300K(x20)
(c)
P_{ex}= 7.5xP_0
8K
20K
30K
60K
70K
80K
100K
120K
140K
160K
180K
200K
240K(x2.5)
300K(x10)
(d)
P_{ex}= 15xP_0
8K
30K
40K
50K
60K
80K
90K
130K
160K
220K(x5)
250K(x10)
300K(x20)
Integrated PL intensity (u. a.)
Energy (eV)
1,0
1,1
1,2
1,3
1,4

Figure 1

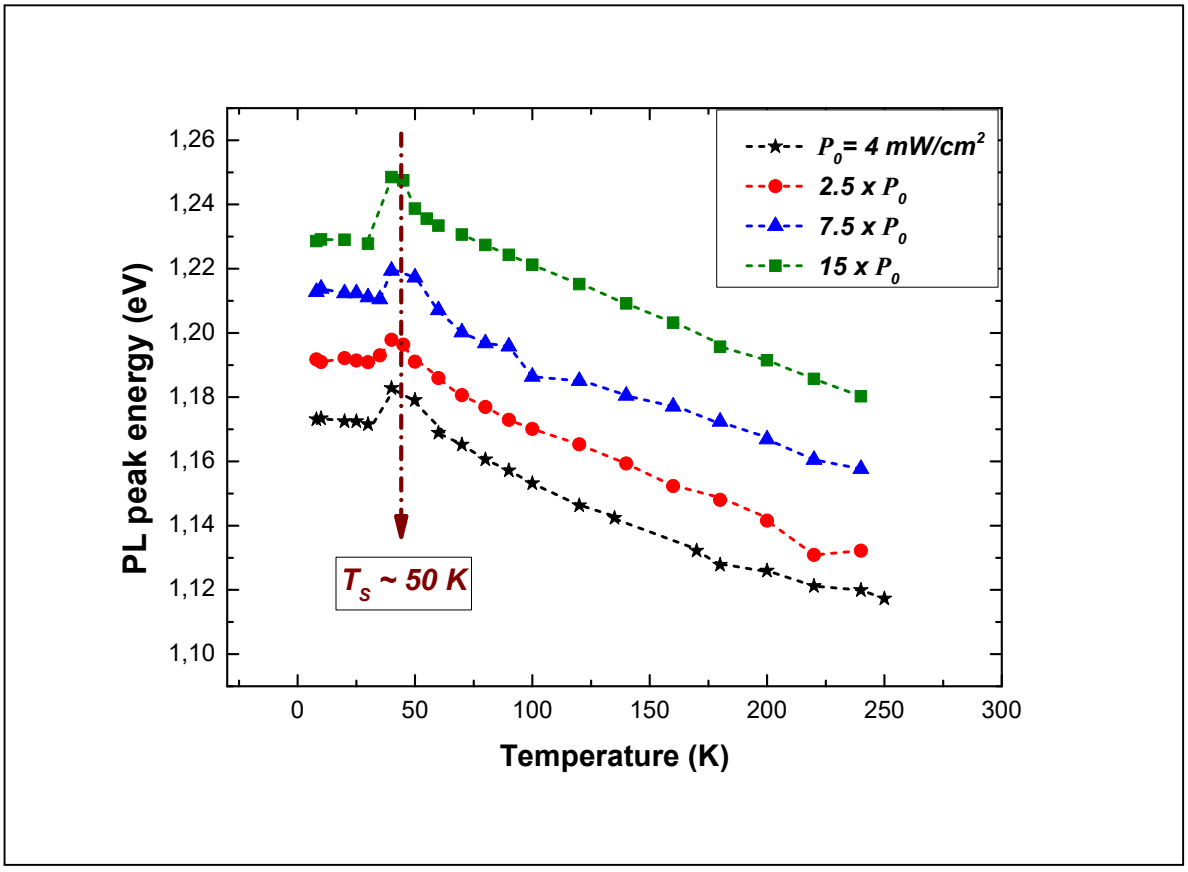
PL peak energy (eV)
1,26
1,24
1,22
1,20
1,18
1,16
1,14
1,12
1,10
0
50
100
150
200
250
300
Temperature (K)
P_0= 4 mW/cm²
2.5 x P_0
7.5 x P_0
15 x P_0
T_S ~ 50 K

Figure 2a

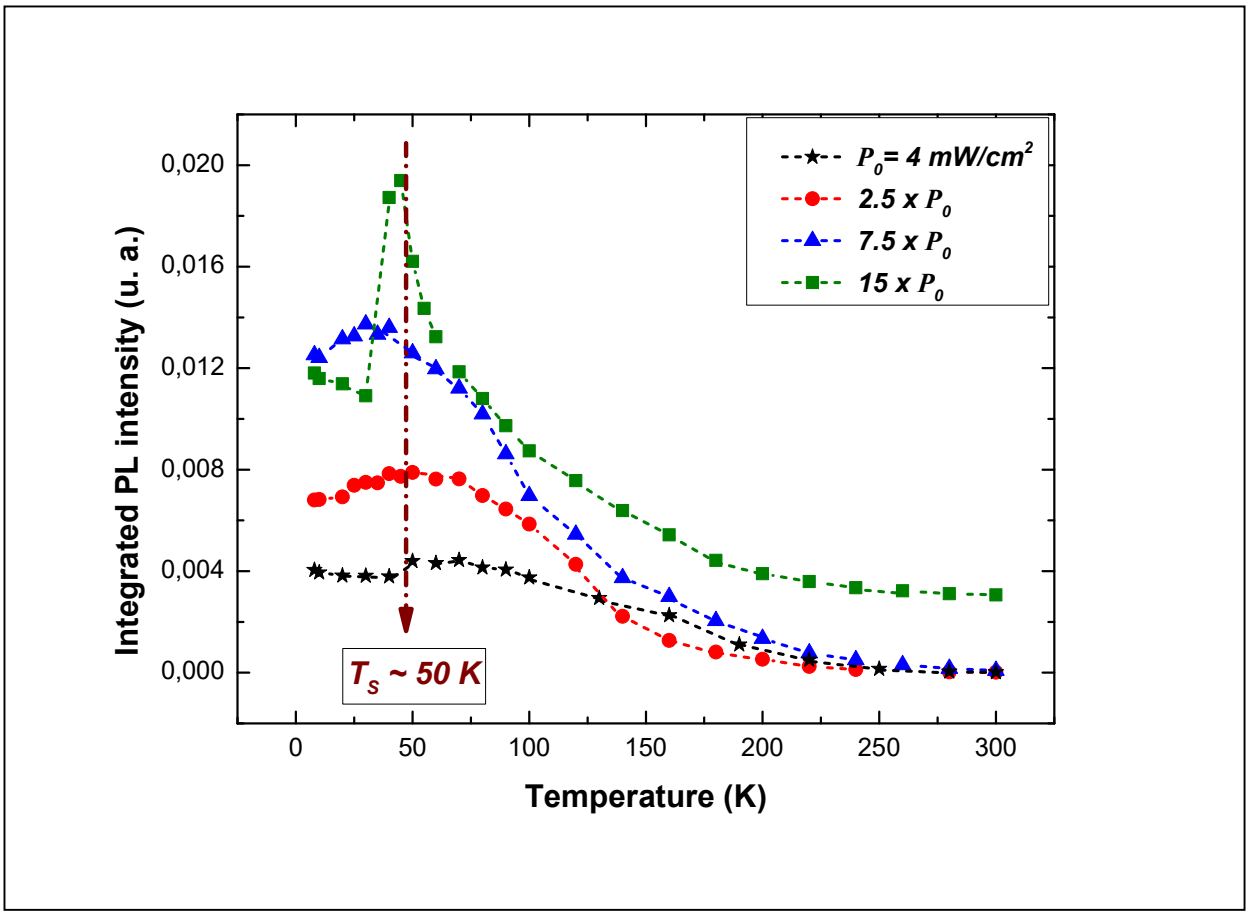
Integrated PL intensity (u. a.)
0,020
0,016
0,012
0,008
0,004
0,000
0
50
100
150
200
250
300
Temperature (K)
P_0= 4 mW/cm^2
2.5 x P_0
7.5 x P_0
15 x P_0
T_S ~ 50 K

Figure 2b

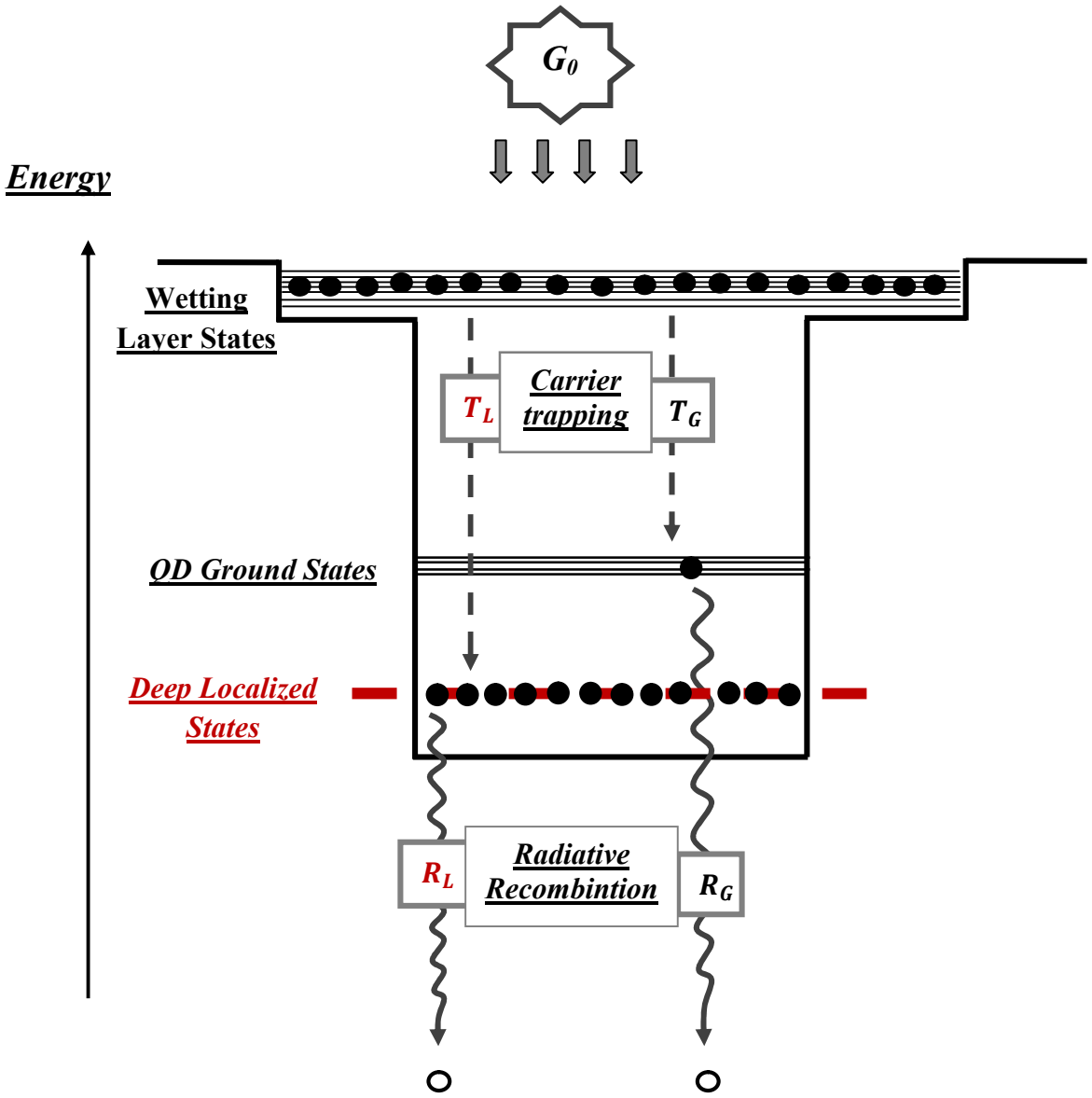

Figure 3 (a): *At very low temperatures (~ 8K).*

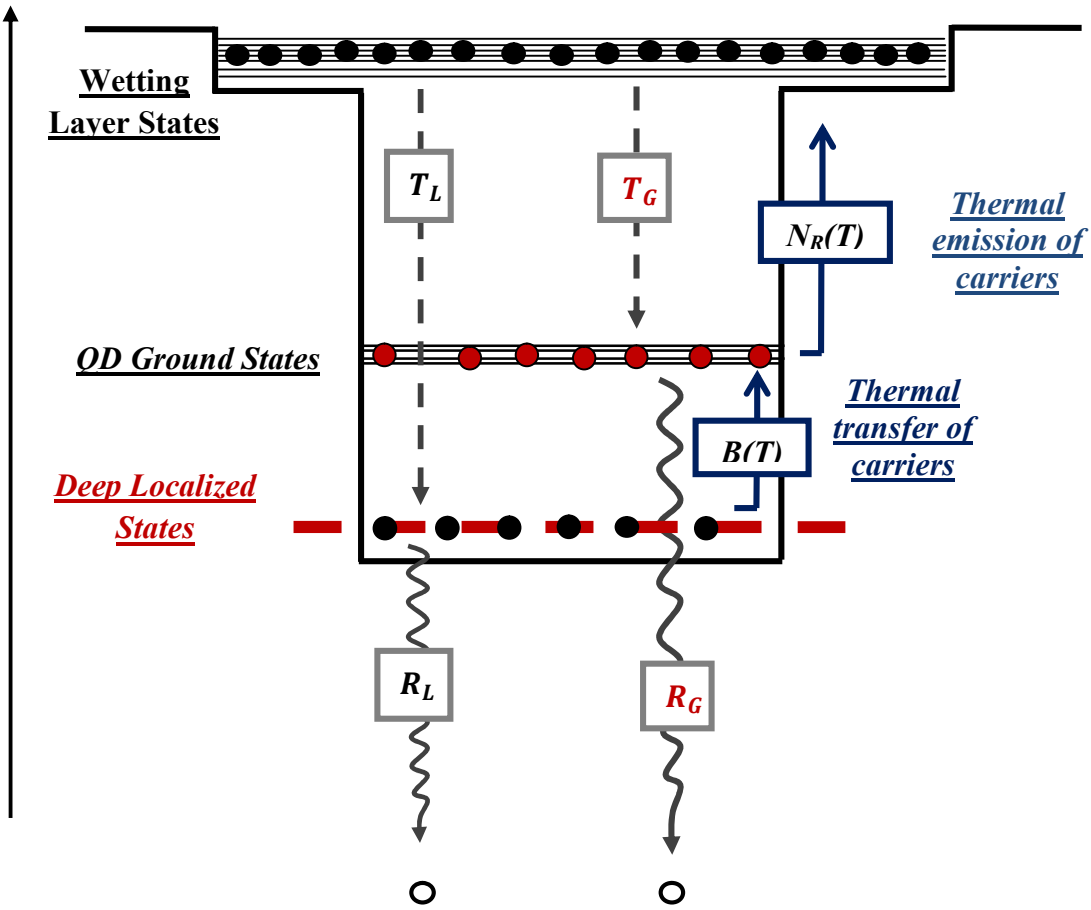

Figure 3 (b): *For temperatures between 8K and T_S.*

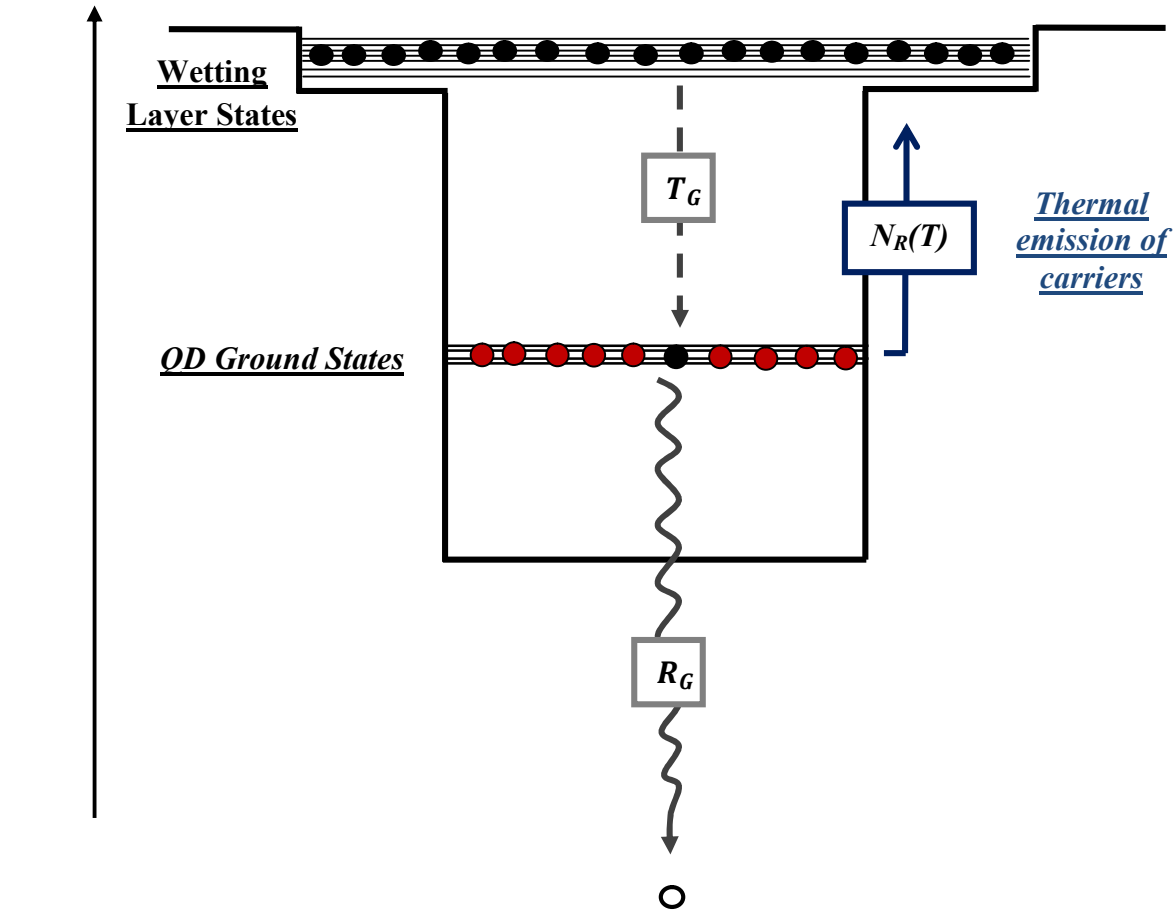

Figure 3 (c): *For temperatures above T_S.*

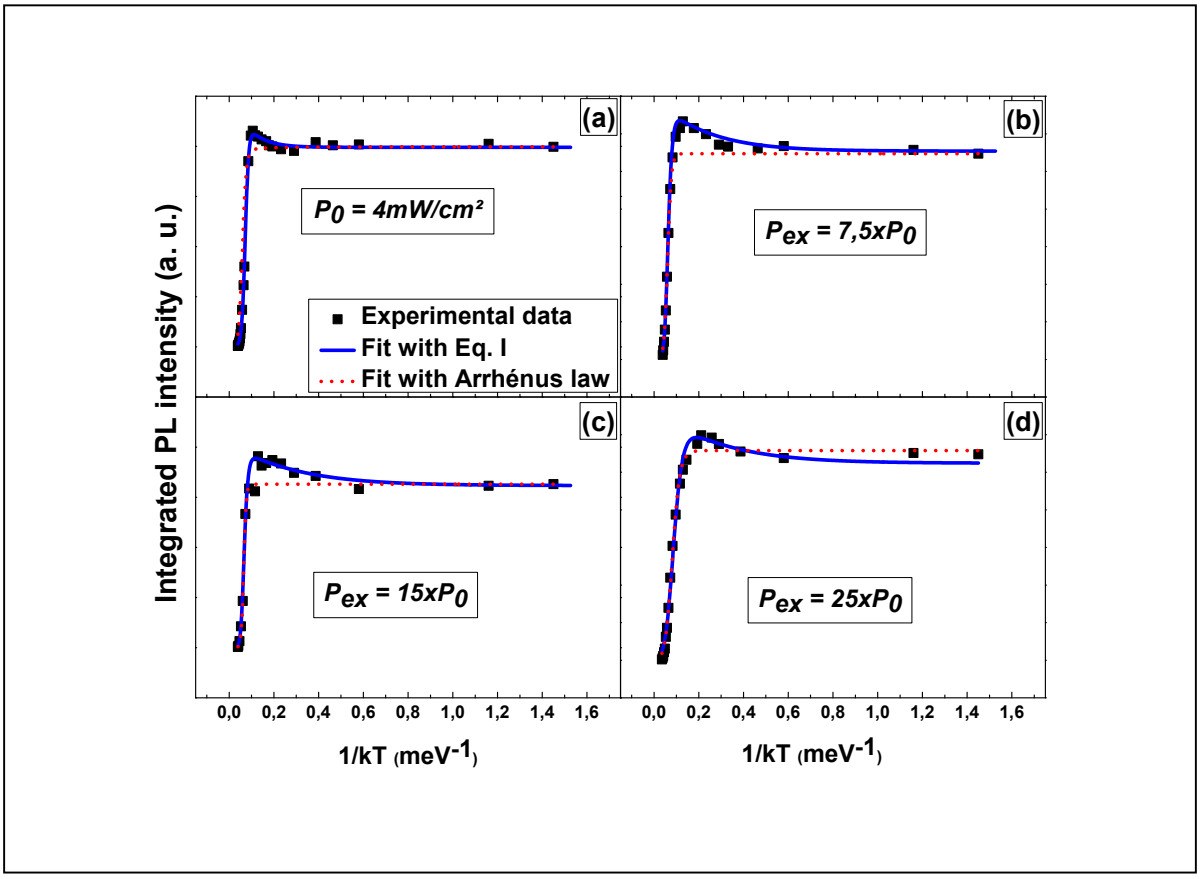
(a)
(b)
(c)
(d)
P_0 = 4mW/cm²
P_{ex} = 7,5xP_0
P_{ex} = 15xP_0
P_{ex} = 25xP_0
Experimental data
Fit with Eq. I
Fit with Arrhénus law
Integrated PL intensity (a. u.)
0,0 0,2 0,4 0,6 0,8 1,0 1,2 1,4 1,6
1/kT (meV^{-1})

Figure 4